available at www.sciencedirect.com

ScienceDirect

www.elsevier.com/locate/brainres

BRAIN RESEARCH

Research Report

Distribution of calbindin-28kD and parvalbumin in V1 in normal adult *Cebus apella* monkeys and in monkeys with retinal lesions

Eliã Pinheiro Botelho[a], *Juliana Guimarães Martins Soares*[a], *Sandra da Silva Pereira*[b], *Mario Fiorani*[a], *Ricardo Gattass*[a,*]

[a]*Laboratório Fisiologia da Cognição, Instituto de Biofísica Carlos Chagas Filho, Universidade Federal do Rio de Janeiro, Brazil*
[b]*Departamento de Otorrino-Oftalmologia, Faculdade de Medicina, Universidade Federal do Rio de Janeiro, Brazil*

ARTICLE INFO

Article history:
Accepted 2 August 2006
Available online 6 September 2006

Keywords:
V1
Cebus monkey
Calcium-binding protein
Calbindin
Parvalbumin
Retinal lesion

ABSTRACT

Several proteins have their normal patterns of distributions altered by monocular visual deprivation. We studied the distribution of the calcium-binding proteins calbindin-28kD (Cb) and parvalbumin (Pv) in V1 in normal adult *Cebus apella* monkeys and in monkeys with monocular retinal lesions. In normal monkeys, the interblobs regions in layers 2/3 and the layer 4B are intensely labeled for Cb, while Pv reaction showed a complementary labeling pattern with a stronger staining in layers 4A, 4C and in the blob regions in layers 2/3. In monkeys with monocular retinal lesion, the laminar distribution of these proteins was differentially affected, although both reactions resulted in stronger labeling in non-deprived ocular dominance columns. While Cb reaction resulted in stronger labeling in layers 1 through 5, Pv labeling was heavier in layers 2/3, 4A and 4C. There was a clear reduction in the intensity of neuropil staining for both Pv and Cb in deprived *ocular dominance* columns with little or no reduction in number of labeled cells. This reduction could thus be attributed to activity-dependent changes at synapses level.

1. Introduction

In the visual system of several species, retinal lesions or long term ocular occlusions promote alterations in the pattern of distribution of many proteins, including the calcium-binding proteins calbindin-28kD (Cb) and parvalbumin (Pv) (Blümcke et al., 1991; Hendry and Bhandari, 1992; Mize et al., 1992b; Blümcke et al., 1994; Carder et al., 1996; Horton and Hocking, 1998; Arckens et al., 2000; Matsubara et al., 2001; Soares et al., 2005). Cb and Pv are cytoplasm proteins members of the EF-hand family of proteins. Each of these proteins can buffer the intracellular calcium ion in specific ways, and they are capable of altering many cellular functions, including the time course of action potentials. They also play a role in the protection of the cells against the damaging effects of excessive calcium influx during prolonged periods of high activity (Heizmann and Hunziker, 1991; Chard et al., 1993; Caillard et al., 2000; Blatow et al., 2003). Previous study showed evidence that both Cb and Pv proteins are important under conditions of N-methyl-D-aspartate (NMDA) receptor activation and consequent calcium influx (Kawaguchi and Kubota, 1993). These conditions are related to plastic changes in the cerebral cortex (Fonta et al., 1997). In primary visual cortex (V1) of adult *Macaque* monkeys, an Old World primate, after monocular visual deprivation, Cb and Pv are differentially reduced in deprived ocular dominance columns,

* *Corresponding author*. Programa de Neurobiologia, Instituto de Biofísica Carlos Chagas Filho, Bloco G, CCS, UFRJ, Ilha do Fundão, Rio de Janeiro, R.J., 21949-900, Brazil. Fax: +55 21 2808193.
E-mail address: rgattass@biof.ufrj.br (R. Gattass).

0006-8993/$ – see front matter © 2006 Elsevier B.V. All rights reserved.
doi:10.1016/j.brainres.2006.08.001

both in number of cells and in neuropil intensity (Blümcke et al., 1994; Gutierrez and Cusick, 1994; Carder et al., 1996).

Studies in V1 of various species of primates showed that these proteins are labeled in different GABAergic cells: Cb is labeled in double-bouquet cells, while Pv is labeled in basket and chandelier cells (DeFelipe et al., 1989a,b; Hendry et al., 1989; Hendry and Carder, 1993). In addition, their laminar distributions in V1 are different and complementary, with no co-localization: Cb labeled cells are mainly found in layers 2/3 while Pv labeled cells and neuropil are mainly observed in layer 4 (Hendry et al., 1989; Blümcke et al., 1994; Johnson and Casagrande, 1995; Carder et al., 1996; Goodchild and Martin, 1998). A similar pattern of labeling has been described in V1 of several non-primate species (Demeulemeester et al., 1989; Celio, 1990; Ichida et al., 2000). Although there are several similarities in the expression of these proteins among different primate species, differences have also been reported (Celio et al., 1986; Hendry et al., 1989; Blümcke et al., 1990, 1991; Hendry and Carder, 1993; Johnson and Casagrande, 1995; Goodchild and Martin, 1998).

In this study, we investigated the distribution of Cb and Pv in V1 of normal adult *Cebus apella* monkeys, a diurnal, medium sized New World primate, comparable in many aspects to the Old World monkey *Macaca fascicularis* (Le Gros Clark, 1959; Freese and Oppenheimer, 1981). Based on brain size, sulcal pattern and diurnal habits, the New World monkey *Cebus* is more comparable to the Old World monkey *Macaca* than to smaller New World monkeys, like *Callithrix* and *Saimiri*, which have smaller and less convoluted brains; furthermore, *Callithrix* and *Saimiri* present differences in the organization of the striate cortex and extrastriate cortex (Gattass and Gross, 1981; Gattass et al., 1981, 1987, 1988, 1990; Rosa et al., 1988, 1992; Fiorani et al., 1989; Sengpiel et al., 1996; Chappert-Piquemal et al., 2001; Rosa, 2002). In addition, we studied the alterations in the distribution of these proteins in V1 of *Cebus* after restricted retinal lesions to investigate the changes in the expression of these calcium-binding proteins caused by lack of normal retinal inputs. Therefore, this study will allow an opportunal comparison of the organization of the visual cortex in normal and deprived New and Old World monkeys, based on similarities and differences on the distribution of the calcium-binding proteins in V1.

2. Results

2.1. *Normal distribution of Pv and Cb*

In V1 of normal adult *Cebus* monkeys, Pv and Cb proteins showed a nearly complementary pattern, both in modular and laminar distributions. Figs. 1A and 2A show the normal pattern of CytOx staining in sections of V1: CytOx is weakly labeled in layer 1, in the interblobs regions in layers 2/3, in layers 4B and 5 and moderately labeled in layer 6. Strong labeling of CytOx is observed in the blobs in layers 2/3 (Figs. 2A and 3A), as well as in layers 4A and 4C. In addition, in Fig. 1A, we can observe that layer 4C can be further divided into two sublayers: 4Cα and 4Cβ. Sublayer 4Cβ occupies the inferior half of layer 4C and is darker than sublayer 4Cα, located in the upper half of layer 4C.

Figs. 1B and 2B illustrate the normal distribution of Pv in V1. Pv distribution follows a pattern similar to CytOx staining, that is, Pv is weakly labeled in layer 1, moderately labeled in layers 2/3, 4B, 5 and 6 and intensely labeled in layers 4A and 4C. Similarly, within layer 4C, sublayer 4Cβ is darker than 4Cα. Using a low gain objective (2.5×) to analyze Pv reacted sections, we note a subtle modular distribution for Pv neuropil in layers 2/3 (Fig. 2B). Comparing each section with the adjacent section reacted for CytOx (Fig. 2A), we observe that Pv neuropil is more intensely labeled in regions which correspond to CytOx blobs (Fig. 2C).

Comparison of the distribution of Cb protein (Fig. 1C) with that of Pv protein (Fig. 1B) shows a nearly complementary distribution for these proteins. The neuropil is intensely labeled for Cb in layer 2 and upper layer 3. We also observe a less intensely labeled neuropil in layer 4B, in the superior half of layer 4Cβ and in a very subtle belt in its inferior limit. Layers 4A, 5 and 6 showed a weakly labeled neuropil, while layer 1 and the inferior portion of layer 3 showed a moderate staining. When analyzing Cb reacted sections with the same gain objective (2.5×) used in the analysis of Pv reacted section, we can also observe a clear modular distribution of neuropil and cell bodies in layers 2/3 (Fig. 3B). The superposition of these sections onto adjacent sections reacted for CytOx shows that Cb is labeled preferentially in regions corresponding to interblobs; however, there is also labeling in some blob regions (Fig. 3C).

In V1 of *Cebus* monkeys, both Pv and Cb labeled multipolar cells, which were, in majority, oval and rounded in shape (Figs. 4 and 5). Pv labeled cells were more numerous in layers 2/3 and layer 4C (Fig. 1B), while Cb labeled cells were more numerous in supragranular layers (Fig. 1C). For both proteins, we found no cell bodies in layer 1 of V1. In this layer, we only observed cellular processes which originate from cells located in lower layers. Pv labeled cells were large (≥12 μm of diameter) and medium sized (≥6 μm and <12 μm of diameter), while Cb labeled cells were medium and small sized (<6 μm of diameter).

Quantitative analysis of the distribution of Pv labeled cells shows that these cells were more numerous in layers 2/3 and layer 4C, mainly in sublayer 4Cβ. Layer 4A had a moderate concentration of these cells, while layers 4B, 5 and 6 had fewer cells. Analysis of Figs. 1B and 2B shows that these cells were homogeneously distributed. Fig. 4A illustrates neurons in layers 2/3, some are heavily labeled while others are lightly stained, with long moderately labeled ascendant and descendant processes. In sublayers 4Cα and 4Cβ, we also observe a difference in relation to cell size: the majority of neurons of sublayer 4Cα are large in size while the neurons of sublayer 4Cβ are of medium size (Fig. 4B). In these sublayers, mainly in sublayer 4Cβ, it is more difficult to see the cellular processes, due to the strong labeling of the neuropil to Pv. Fig. 4C shows neurons from layers 5 and Fig. 4D shows layer 6 with neurons concentrated in its upper part.

In contrast, the quantitative analysis of Cb labeled cells shows that these cells were more numerous in layer 2, moderate in number in layers 3 and 5 and scarce in layers 4A, 4B, 4C and 6. In layers 2 and 3, as illustrated in Fig. 3B, these neurons are more concentrated in the interblobs regions. In layer 4A, we found few, sparsely distributed, intensely and lightly labeled neurons, while in layers 4B and 4C we observed a large number of lightly labeled neurons and few moderately labeled neurons homogeneously distributed throughout these layers. In Fig. 5A, we can see neurons in layer 2 with long

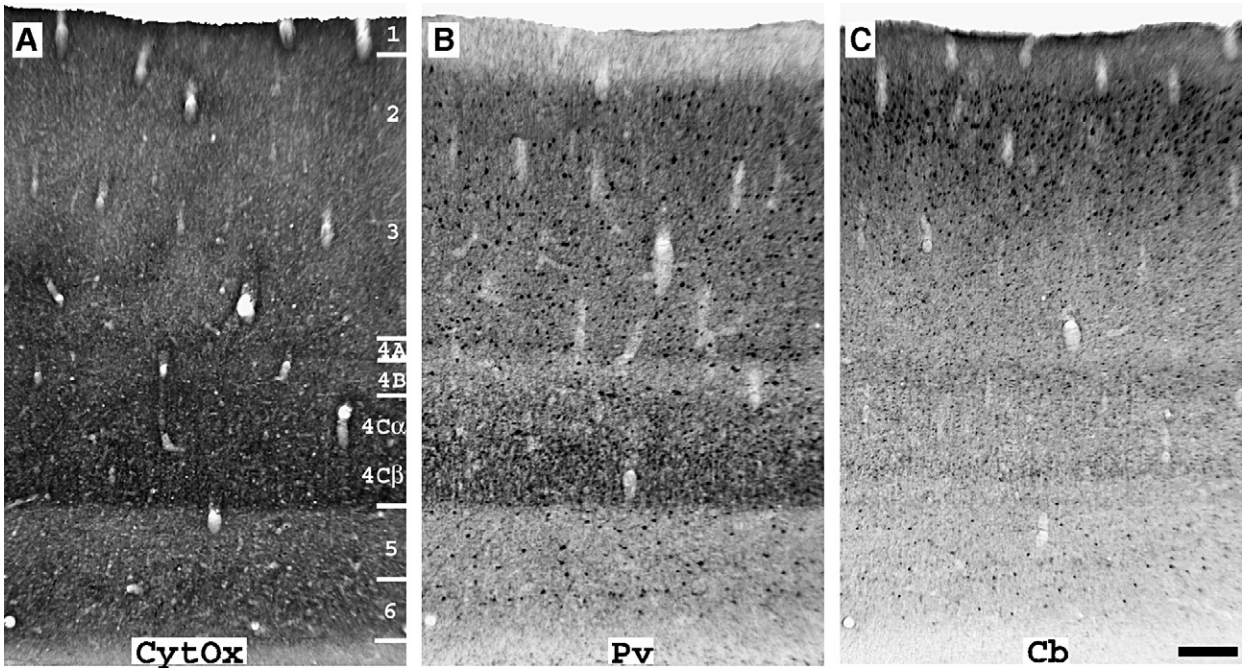

Fig. 1 – Photomicrographs of adjacent coronal sections of V1 of adult normal *Cebus* stained for cytochrome oxidase (CytOx) (A), Pv (B) and Cb (C). In A, the layers of V1 are delineated. Note the similarity of CytOx and Pv staining and a near complementary distribution of Pv and Cb. Scale bar = 500 μm.

intensely labeled ascendant and descendant processes. Fig. 5B depicts moderately labeled cells and the stumps of their cellular processes in layers 4B and 4C. In layers 5 and 6, we observe moderately labeled neurons with long horizontal cellular processes and long ascendant and descendant processes, as illustrated in Figs. 5C and D.

2.2. *Distribution of Pv and Cb after retinal lesion*

Fig. 6A shows a coronal section of V1 of one of the animals with retinal lesion stained for Pv. The comparison of Fig. 6A with B shows that the pattern of distribution for Pv is similar to that of CytOx, where there is a reduction in the staining density in the blobs in layers 2/3 as well as in layers 4A and 4C, in regions corresponding to the dODCs. The densitometric analysis for Pv protein in all V1 layers, comparing ndODCs with dODCs, shows a significant reduction ($p \leq 0.05$) in the density for dODCs in layers 2/3, 4A and 4C, which corroborates our qualitative analysis (Fig. 7A). Similar to Pv staining, Cb staining was also reduced in dODCs, however, with a different pattern of laminar distribution: it occurred from layer 1 to layer 5, as illustrated in Fig. 6C. This result was also confirmed by densitometric analysis in all V1 layers, comparing ndODCs with dODCs ($p \leq 0.05$) (Fig. 7B).

We also quantified these results to verify whether the density reduction was due to a decrease in the intensity of the neuropil or in the number of cells labeled for these proteins, in layers where we found a significant difference in the density of stain for both proteins. The quantitative analysis for Pv labeled cells showed that, in layers 2/3, 4A and 4C, there is no significant difference in the number of labeled cells when comparing ndODCs with dODCs ($p \geq 0.05$) (Fig. 7C). We also compared the numbers of Cb labeled cells in layers 2 through 5, and we found more Cb labeled cells in ndODCs than in dODCs ($p \leq 0.05$) (Fig. 7D). Therefore, we suggest that the decreased density for Pv is a result of a reduction in the intensity of labeling of the neuropil in dODCs in layers 2/3, 4A and 4C, while that for Cb is due to a reduction both in neuropil intensity, from layer 1 through 5, as well as in the number of Cb labeled cells, from layer 2 to layer 5, in dODCs.

Based on these data, we can conclude that the pattern of distribution of Pv protein is similar to that of CytOx in V1 of *Cebus* monkeys. Pv and Cb proteins labeled different populations of neurons with distributions which are nearly complementary. Pv is more intensely labeled in blobs in layers 2/3, layers 4A and 4C, while Cb is more intensely labeled in the interblobs regions in layers 2/3 and in layer 4B and very weakly labeled in layers 4A, 5 and 6. Furthermore, these proteins are differentially affected by retinal lesion inasmuch as for Pv we observe a reduction in the intensity of neuropil, and for Cb, in addition to the reduction in neuropil intensity, we also observe a reduction in the number of labeled cells.

3. Discussion

3.1. *The normal distribution of Cb and Pv*

In general, calbindin and parvalbumin have a complementary distribution throughout the layers of V1 and are found in different populations of cells in *Cebus*, in other primate species (*Macaca*: Hendry et al., 1989; Hendry and Carder, 1993; Carder et al., 1996; *Samiri sciureus*: Celio et al., 1986; Hendry and Carder, 1993; *Galago crassicaudatus*: Johnson and Casagrande, 1995;

Callithrix jacchus: Goodchild and Martin, 1998), as well as in many other non-primate species (cats: Demeulemeester et al., 1989; rats: Celio, 1990; flying fox: Ichida et al., 2000).

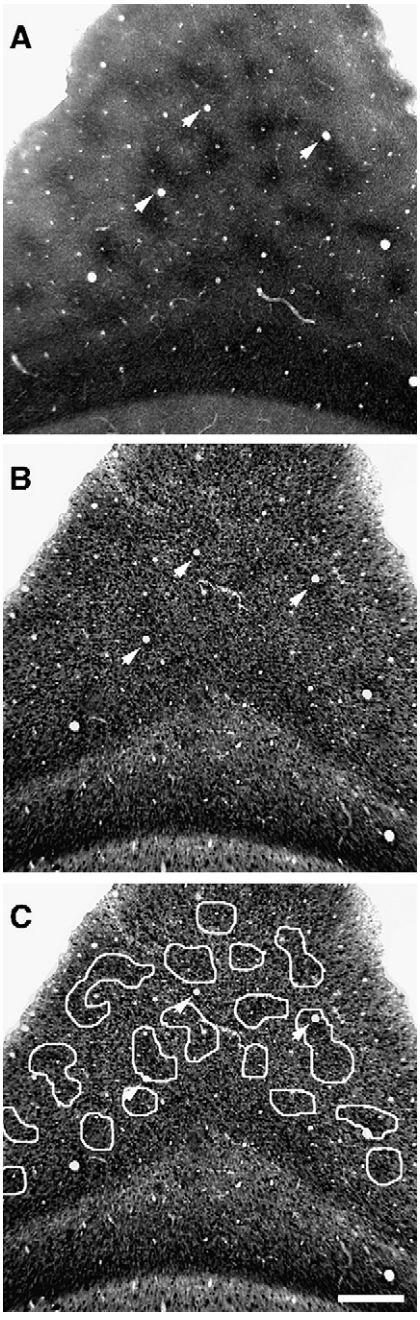

Fig. 2 – Photomicrographs of adjacent parasagittal sections through V1 of normal adult *Cebus*. (A) CytOx staining showing the blobs in layers 2/3 and an intense labeling in layers 4A and 4C. (B) Immunostain for Pv protein depicting a neuropil labeling pattern similar to that of CytOx. (C) Superposition of the section stained for CytOx with the section immunostained for Pv. The regions corresponding to the CytOx blobs are represented by the white traces. As we can note, neuropil labeling to Pv is more intense in the blob regions. The arrowheads point to the blood vessels used in the superposition of the adjacent sections. Scale bar=500 μm.

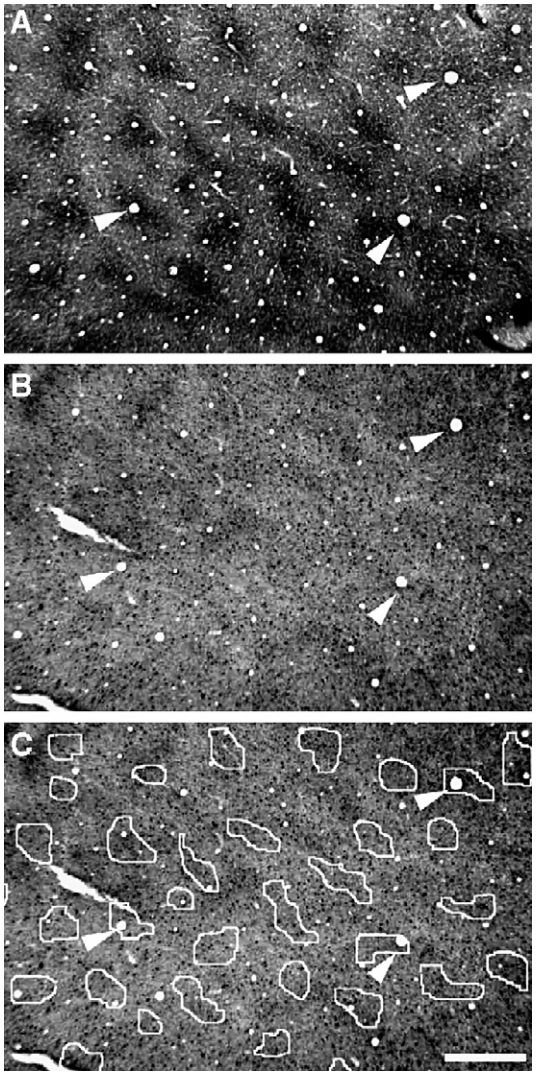

Fig. 3 – Photomicrographs of adjacent tangential sections through V1 of normal adult *Cebus* monkey. (A) Blobs of CytOx in layers 2/3 and (B) normal labeling pattern to Cb protein in layer 3. (C) Superposition of the section stained for CytOx with the section immunostained for Cb. The regions corresponding to the CytOx blobs are represented by the white traces. As we can observe, Cb preferentially labels the interblobs regions, but it also labels some blobs. The arrowheads point to the blood vessels used in the superposition of the adjacent sections. Scale bar=500 μm.

However, although there are several similarities in the expression of these proteins, in the New World monkey *Cebus*, we found specific differences in the pattern of distribution of calbindin throughout the layers of V1 when comparing our results with those of both the Old World monkey *Macaca* or the New World monkey *Saimiri*. In *Cebus* monkey, we found medium and small, heavily stained calbindin-positive neurons concentrated in layers 2/3 and 5 and a dense labeling of neuropil in the interblobs regions in layer 2 and upper layer 3. In this aspect, the labeling pattern for calbindin in *Cebus* resembles more that described for the Old World monkey *Macaca* (Hendry et al., 1989) than that described for the New

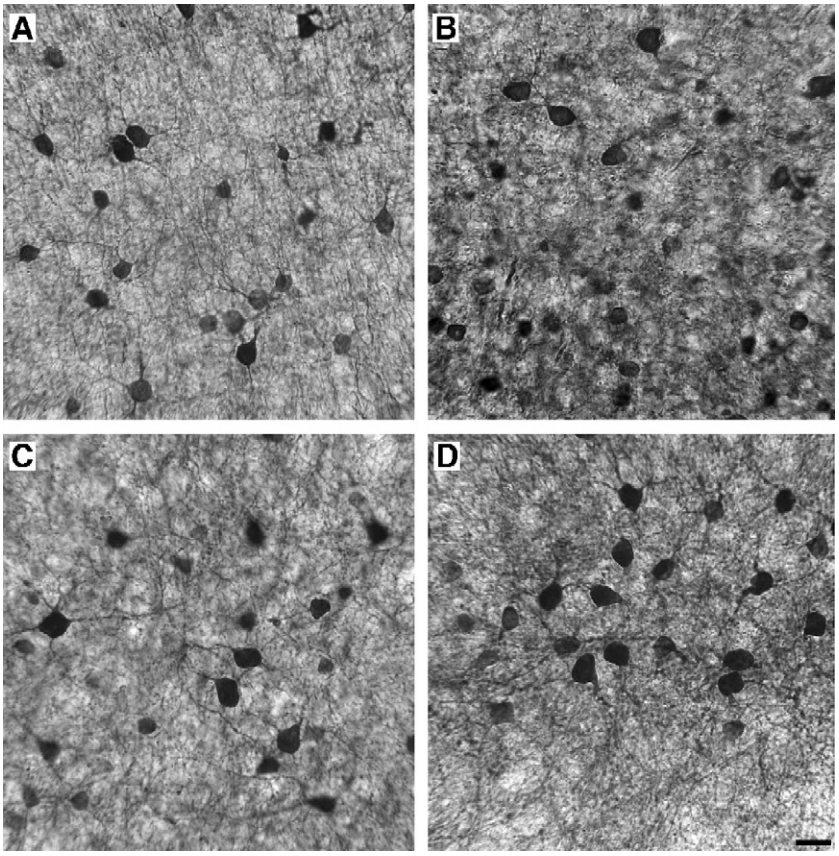

Fig. 4 – High power photomicrographs of coronal sections of V1 of normal adult *Cebus apella* monkey showing cells labeled for Pv in layers 2/3 (A), 4C (B), 5 (C) and 6 (D). We can note large and round cell bodies in sublayer 4Cα and medium cell bodies in sublayer 4Cβ. In all layers, we can observe moderately labeled ascendant and descendant processes. Scale bar=20 μm.

World monkey *Saimiri* (Celio et al., 1986; Hendry and Carder, 1993) or *Callithrix* (Goodchild and Martin, 1998). In *Saimiri*, calbindin intensely labeled neurons and neuropil have also been observed in layers 4Cα (Celio et al., 1986), or 4B (Hendry and Carder, 1993), 5 and 6 (Celio et al., 1986; Hendry and Carder, 1993) forming a matrix that surrounds the cytochrome oxidase blobs. In *Callithrix*, there is a high density of calbindin immunoreactive neurons and neuropil in laminae 2, 3, 4A and 4C (Goodchild and Martin, 1998).

In this study, the immunohistochemistry for parvalbumin labeled mainly medium and large multipolar neurons in layers 2–6, but mainly in layers 2/3 and 4C. Layers 4A and 4C presented a homogeneously heavy labeled neuropil, while in layers 2/3 the labeling of neuropil was more intense in blob regions, with a pattern similar to that evidenced by cytochrome oxidase reaction. This labeling pattern for parvalbumin, mainly in geniculo-recipient layers and compartments of V1, is similar to that described for other primates (Hendry et al., 1989; Blümcke et al., 1990; Johnson and Casagrande, 1995; Goodchild and Martin, 1998).

3.2. *Pv and Cb distribution after monocular visual deprivation*

In this study, we observed a decrease in neuropil intensity for both Cb and Pv in the ocular dominance columns related to the lesioned eye. However, for Cb staining, we found, in addition, a decrease in the number of labeled cells in monkeys with retinal lesions. For Pv staining, our results are similar to the results described by Blümcke et al. (1994) in *Macaca* after monocular enucleation, but differ from those described by Carder et al. (1996), using inactivation by TTX. These authors found not only a reduction in neuropil but also a decrease in the number of labeled cells in the dODCs after 20 days of monocular inactivation. On the other hand, for Cb staining, our results are similar to those described by Carder et al. (1996) inasmuch as they described a reduction in neuropil intensity and in the number of cell bodies in all V1 layers and different from those described by Blümcke et al. (1994) who observed reduction in neuropil intensity from layer 1 to layer 5 and reduction in the number of labeled cells only in layers 2/3 and in the merge between layer 4B and 4Cα. In addition to interspecies differences, these different results could be due either to the different methods used in these studies (monocular enucleation vs TTX vs restricted retinal lesion) or to the use of different antibodies as previously suggested by Carder et al. (1996).

The reduction of Cb and Pv staining in the neuropil in the dODCs could be related either to axonal degeneration or to a decreased transport of these proteins to the neuropil, due to a reduction of production of these proteins in the cellular bodies. Blümcke et al. (1994) suggested that this reduction

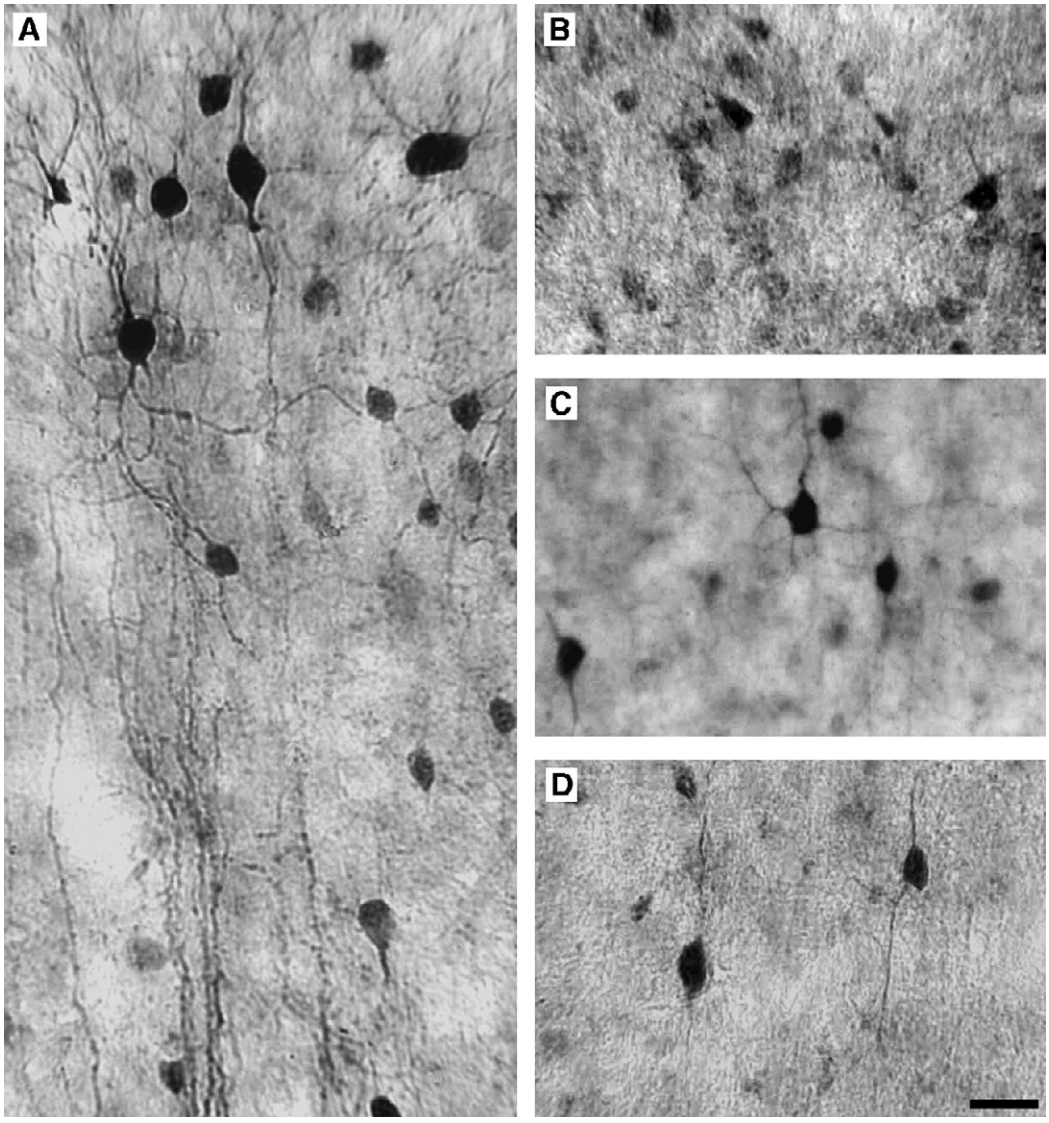

Fig. 5 – High power photomicrographs of coronal sections through V1 of normal adult *Cebus apella* monkey showing cells labeled for Cb. (A) Cells in layers 2 and 3 with long intensely labeled ascendant and descendant processes. (B) In layer 4B, we observe numerous lightly labeled cells and few cells intensely labeled with moderately labeled process stumps. Cells in layers 5 (C) and 6 (D) show long horizontal and vertical moderately labeled processes. Scale bar = 20 μm.

could be due to a centripetally redistribution of these protein, that is, they would migrate from the neuropil towards the cell bodies. However, similarly to what had been described by Carder et al. (1996), we observed not only a decreased labeling for Cb staining in the neuropil in regions corresponding to dODCs, but also a decrease in the number of Cb labeled cells in these regions. Therefore, these findings could be related to alterations in Cb protein epitope promoted by the withdrawal of retinal inputs, similar to what has been proposed by Blümcke et al. (1994). Another plausible explanation could be that the level of intracellular Cb protein is very low such that the labeling could not be observed in these bodies.

The different alterations observed for Pv and Cb staining after retinal lesions could be related to structural differences in these proteins (Heizmann and Hunziker, 1991; Chard et al., 1993). The differences in dendritic arborizations of Cb and Pv labeled cells (DeFelipe et al., 1989a,b; Hendry et al., 1989; Hendry and Carder, 1993) could implicate in that they may receive different inputs, therefore leading to different alterations after retinal lesion, as suggested by Carder et al. (1996). Other studies have shown that these proteins are differentially affected by various factors such as different methods of studies (Mize et al., 1992b; Blümcke et al., 1994; Carder et al., 1996), age at the onset of deprivation, duration of deprivation (Cellerino et al., 1992; Mize et al., 1992b; Blümcke et al., 1994; Carder et al., 1996), difference in reactivity of different areas of the central nervous system (Rausell et al., 1992) and species studied (Cellerino et al., 1992; Blümcke et al., 1994; Carder et al., 1996).

3.3. *Probable roles of Cb and Pv*

The precise functions of the calcium-binding proteins are still unknown. Pv staining is generally found associated with

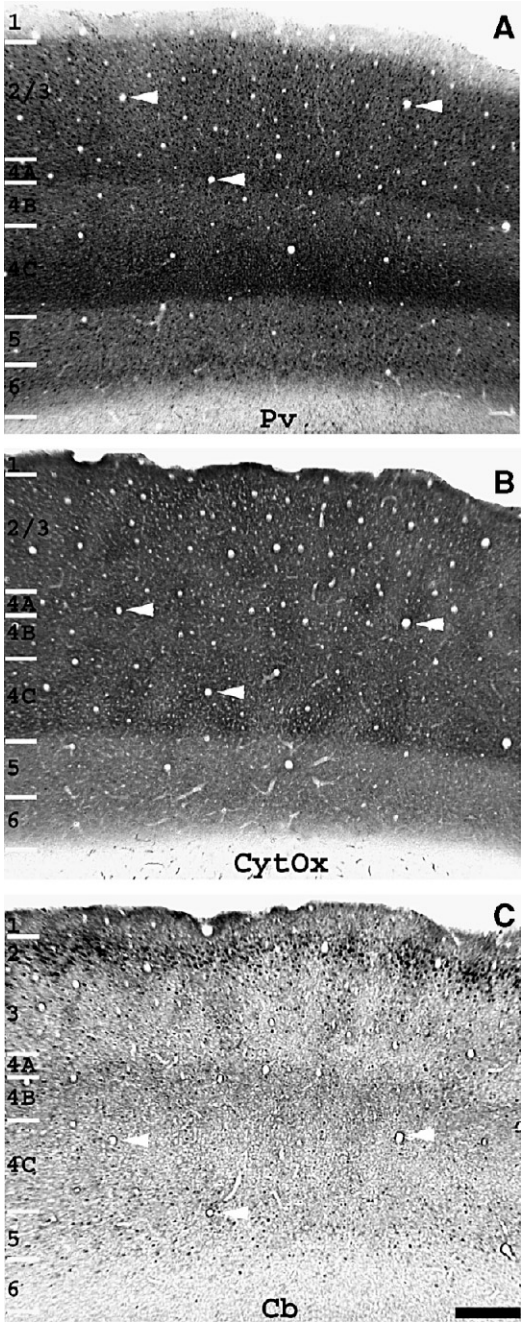

Fig. 6 – Photomicrographs of coronal sections of V1 of one adult *Cebus* monkey with monocular retinal lesion. (A) Section immunoreacted for Pv showing a decrease in the staining for this protein in dODC in layers 2/3, 4A and 4C. (B) Adjacent section stained for CytOx, illustrating the dODC (light bands) and ndODC (dark bands) in layer 4C. (C) Adjacent section reacted for Cb showing a reduction in the staining of this protein from layer 1 to layer 5 in dODC. The arrowheads point to the blood vessels used in the superposition of the sections. Scale bar = 500 μm.

cells that are more active metabolically. Physiological studies in frontal cortex of rats showed that Pv labeled neurons are GABAergic, fast-spiking cells that fire repetitively with almost no adaptation, whereas Cb labeled neurons are GABAergic cells that produce low-threshold spikes from hyperpolarized potentials and show spike-frequency adaptation (Blümcke et al., 1990; Kawaguchi and Kubota, 1993). In the cerebral cortex of monkeys, immunoreactivity for calbindin and parvalbumin has been described to be localized within distinct sub-populations of GABAergic interneurons (Celio et al., 1986; Hendry et al., 1989). However, whereas the occurrence of Pv staining is restricted to GABAergic neurons, Cb staining may also be found in non-GABAergic pyramidal neurons (Van Brederode et al., 1990; DeFelipe and Jones, 1992). In the LGN of cats, the vast majority of Pv labeled neurons also showed GABA immunoreactivity (Stichel et al., 1988). On the other hand, in the monkey thalamus, most parvalbumin and calbindin labeled cells are not GABAergic, and both cells appear to be relay neurons (Jones and Hendry, 1989; Tigges and Tigges, 1991; Mize et al., 1992b; Soares et al., 2001). In superior colliculus of cat, Pv labeled neurons are mostly projection neurons. Most Cb labeled cells are interneurons, but only a few Cb labeled neurons contain GABA and a significant fraction of cells in the superficial tier project to the LGN (Mize et al., 1991, 1992a). Therefore, these proteins appear to be used in distinct manners by different cell populations in the cortex and subcortical nuclei. Hendry and Jones (1986) showed that in *Macaca* the staining for GABA and GAD in layers 4C and 4A was reduced 2 weeks after eye removal, in both neuronal somata and terminals within columns associated with the removed eye, which suggests that the GABA concentration in cortical neurons may depend on their levels of activity.

Cortical reorganization has been related with intrinsic cortical alterations, such as decrease or increase in the strength of connections, which can involve sprouting of axons of long-range laterally projecting neurons, as well as synaptogenesis (Gilbert and Wiesel, 1992; Darian-Smith and Gilbert, 1994, 1995; Chino, 1995; Rosa et al., 1995). Caillard et al. (2000) showed that these proteins can modulate short term plasticity, where Pv promotes a synaptic depression, and Blatow et al. (2003) showed that the washout of Cb from multipolar bursting cells abolishes synaptic facilitation. The reduction of the neuropil staining for both Pv and Cb in the deprived columns with little or lack of decrease in the labeling in neuronal somata can be due to activity-dependent changes occurring at synapses level in terminals of geniculocortical projection cells or of cortical interneurons in V1.

4. Experimental procedures

In this study, we used 6 adult *C. apella* monkeys weighing 2–3 kg. All experimental protocols were conducted following the NIH guidelines for animal research and were approved by the committee for animal care and use of the Instituto de Biofísica Carlos Chagas Filho, UFRJ. Two of these animals received focal laser retinal lesions in the right eye.

Before the retinal lesion, each animal was anesthetized with intramuscular administration of 0.5 ml/kg of a 1:4 mixture of 6% Ketamine hydrochloride (Ketalar; ParkeDavis) and 2% Dihydrotiazine hydrochloride (Rompum; Bayer). Atropine sulfate (0.15 mg/kg) and benzodiazepine (0.8 mg/kg) were intramuscularly injected to prevent tracheobronchic

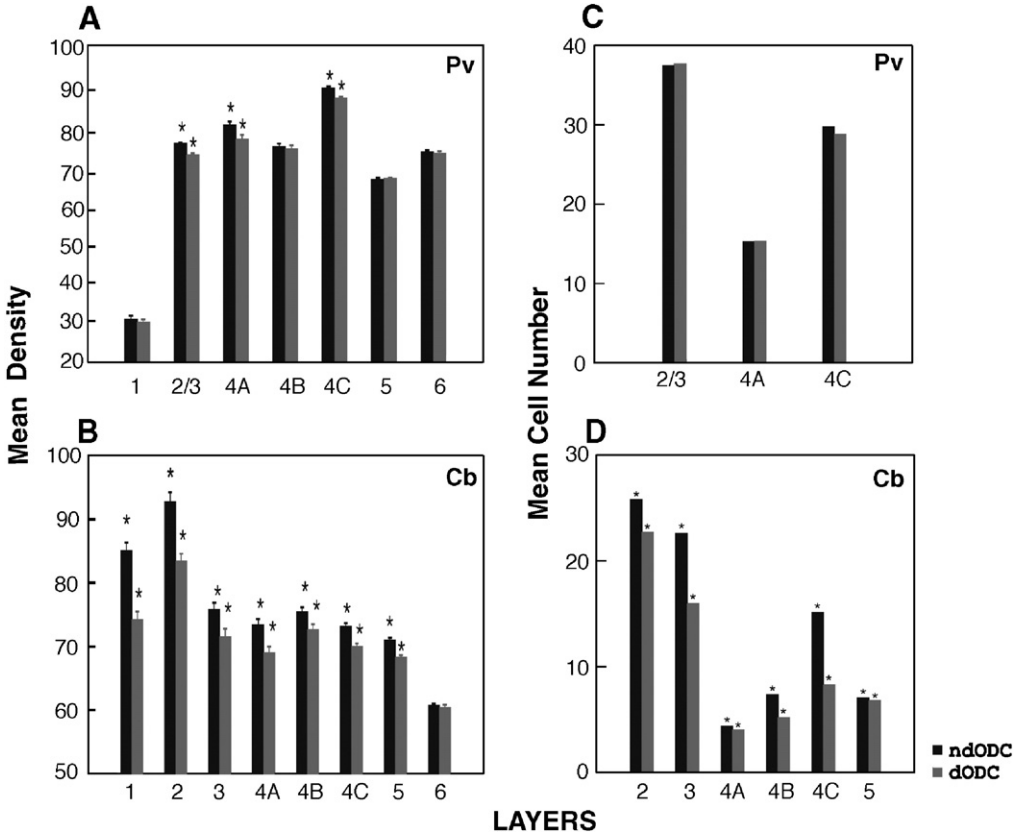

Fig. 7 – Mean density of the ocular dominance columns labeled for Pv (A) and Cb (B) and mean of the number of cells labeled for Pv (C) and Cb (D) in V1 in the region corresponding to the retinal lesion. The densitometric analysis was done in all layers of V1. Pv labeled cells were counted in layers 2/3, 4A and 4C (C) and Cb labeled cells were counted in layers 2, 3, 4A, 4B, 4C and 5 (D). The black bars represent the ndODC and the gray bars represent the dODC. Error bars = standard error. * = statistically significant difference.

secretion and stress, respectively. The pupil was dilated with 1% tropicamide and 10% phenylephrine hydrochloride. Retinal lesions were made on the temporal margin of the optic disc, in the right eye, using 5 shots of Neodymium-YAG laser with the potency of 0.8 mW and 0.1 s duration. These lesions affected all foveal representation in the visual field (approximately 2°) and resulted in a complete destruction of all ganglionar cell fibers crossing the lesioned region (Fig. 8). The effect of the retinal lesions was confirmed by cytochrome oxidase (CytOx) reaction in V1 in retinotopically corresponding region, where we observed alternate dark and light bands in layer 4C, which correspond to the normal, or non-deprived ocular dominance columns (ndODCs), and the lesioned eye, or to the deprived ocular dominance columns (dODCs), respectively (see Fig. 6B). After a 28-day survival time, the animals were transcardially perfused.

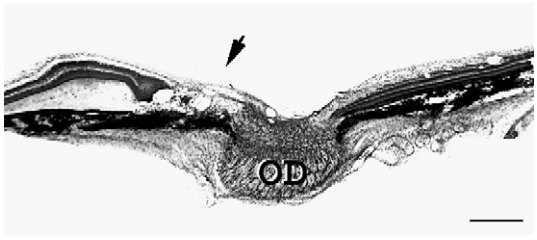

Fig. 8 – Photomicrograph of a horizontal retinal section, through the optic disc (OD), stained with neutral red. The arrow points to the lesion where we can observe all retinal layers destroyed. Scale bar = 500 μm.

Before perfusion, all animals were initially anesthetized with intramuscular administration of 6% Ketamine hydrochloride (Ketalar; ParkeDavis, 30 mg/kg) followed by an intravenous lethal dose of sodium pentobarbital (30 mg/kg). All animals were perfused with saline 0.9%, followed by 4% paraformaldehyde in phosphate buffer saline (PBS), then by 4% paraformaldehyde in PBS + 2.5% glycerol and finally with increasing concentrations of glycerol solution (5% and 10%) in PBS.

After perfusion, the brains and the eyes with the lesion were removed for histological processing. The retinas were blocked, cut in the horizontal plane at 30 μm thickness on a cryostat, stained with neutral red and examined under light microscopy to verify the efficiency of the lesion. Serial coronal sections of the brains were obtained with a cryostat at 40 μm thickness. Adjacent series were stained for cell bodies with cresyl violet and reacted for CytOx histochemistry (Silvermann and Tootell, 1987) and for immunocytochemistry for Pv and Cb. For the immunocytochemical

reactions, sections were initially incubated for 16 h, at room temperature, in mouse monoclonal anti-Cb (1:2000) and anti-Pv (1:2500) (Bellinzona, Switzerland) in phosphate buffer saline diluted 10× (PBSb) followed by an additional incubation, at room temperature, in biotynilated anti-mouse secondary antibody made in horse (1:200, Vector, Burlingame, CA) for 90 min. The sections were then processed following the avidin–biotin method, with ABC kits (Vector, Burlingame, CA) and 0.05% diaminobenzidine. Finally, the sections were rinsed in PBSb and mounted on gelatin-coated-slides, dehydrated and cover-slipped. Control sections were prepared by omitting the primary antibody in the incubation solution. These sections showed no specific staining. For each animal, all sections were simultaneously immunoreacted in a single battery to minimize variability in the reaction product among different immunoruns.

To analyze the normal distributions of Cb and Pv proteins, the images of normal sections labeled for Nissl and CytOx and of adjacent sections reacted for Cb and Pv were examined under light microscopy with small gain objectives (2.5× and 6.3×) using an Axio Cam camera (Carl Zeiss), attached to a Leitz Ortoplan microscope interfaced with a PC. The images of the sections were then aligned using Adobe Photoshop 6.0 software. Images of CytOx and Nissl stained sections were superimposed onto images of adjacent Cb and Pv stained sections. The Cb and Pv stained sections superimposed onto adjacent Nissl stained sections allowed the study of the laminar distribution of these proteins in V1, while those superimposed onto CytOx stained sections allowed the analysis of their modular distribution.

To quantify the intensity of the reactions for Cb and Pv proteins in different ocular dominance columns in animals with monocular lesions, images of adjacent sections reacted for CytOx, Cb and Pv were analyzed using the same system employed for studying the normal distribution. For each animal ($n=2$), we made densitometric analysis in three sections labeled for Pv and in three additional sections labeled for Cb. In each section, for each V1 layer, we selected five regions of Cb or Pv images corresponding to dODCs ($n=15$) and ndODCs ($n=15$) of CytOx images. Then, we submitted these fragments of the images to an Image Analyzer Program (Image Scion). To allow promediation of the data, the absorbance indices obtained in this analysis were transformed into percentages, taking the maximum density value of the reaction, in each section, as 100%.

In order to verify whether the density alterations found in the densitometric analysis between dODCs and ndODCs were due to a reduction in the number of cells or in the intensity of the neuropil, we photomicrographed three sections reacted for Cb and three for Pv using a 6.3× microscopy objective. After this procedure, we counted manually all cellular bodies in a rectangular area centered both in dODCs ($n=15$) and in ndODCs ($n=15$) in the different layers in order to determine the cell density for each layer. These rectangular areas measured 30.240 μm^2 for layers 2, 5 and 6, 100.320 μm^2 for layers 3 and 4C and 8.360 μm^2 for layer 4A.

The absorbance index and the number of cells data were submitted to statistical analysis. Analysis of variance (ANOVA) and Tukey post hoc testing were used for multiple comparisons and paired *t* test for simple comparisons.

Acknowledgments

The authors are grateful to Dr. Aglai Penna Barbosa de Souza for comments on the manuscript, Dr. Sheila do Nascimento Silva for helping with the figures, Edil Saturato, Liliane Heringer, Paulo Coutinho, Gervásio Coutinho and Thereza Monteiro for their technical support. This research was supported by grants from the following institutions: CNPq, FAPERJ and FUJB.

REFERENCES

Arckens, L., der Gucht, E.V.D, Eysel, U.T., Orban, G.A., Vandesande, F., 2000. Investigation of cortical reorganization in area 17 and nine extrastriate visual areas through the detection of changes in immediate early gene expression as induced by retinal lesions. J. Comp. Neurol. 425, 531–544.

Blatow, M., Caputi, A., Burnashev, N., Monyer, H., Rozov, A., 2003. Ca^{2+} buffer saturation underlies paired pulse facilitation in calbindin-D28k-containing terminals. Neuron 38, 79–88.

Blümcke, I., Hof, P.R., Morrison, J.H., Celio, M.R., 1990. Distribution of parvalbumin immunoreactivity in the visual cortex of Old World monkeys and humans. J. Comp. Neurol. 301, 417–432.

Blümcke, I., Hof, P.R., Morrison, J.H., Celio, M.R., 1991. Parvalbumin in the monkey striate cortex: a quantitative immunoelectron-microscopy study. Brain Res. 554, 237–243.

Blümcke, I., Weruaga, E., Kasas, S., Hendrickson, A.E., Celio, M.R., 1994. Discrete reduction patterns of parvalbumin and calbindin D-28k immunoreactivity in the dorsal lateral geniculate nucleus and the striate cortex of adult macaque monkeys after monocular enucleation. Visual Neurosci. 11, 1–11.

Caillard, O., Moreno, H., Schwaller, B., Llano, I., Celio, M.R., Marty, A., 2000. Role of the calcium-binding protein parvalbumin in short-term synaptic plasticity. Proc. Natl. Acad. Sci. U. S. A. 97, 13372–13377.

Carder, K.R., Leclere, S.S, Hendry, S.H.C., 1996. Regulation of calcium-binding protein immunoreactivity in GABA neurons of macaque primary visual cortex. Cereb. Cortex 6, 271–287.

Celio, M.R., 1990. Calbindin D-28k and parvalbumin in the rat nervous system. Neuroscience 35, 375–475.

Celio, M.R., Scharer, L., Morrison, J.H., Norman, A.W., Bloom, F.E., 1986. Calbindin D-28k immunoreactivity alternate with cytochrome oxidase rich-zones in some layers of the primate visual cortex. Nature 323, 715–717.

Cellerino, A., Siciliano, R., Dmenici, L., Maffei, L., 1992. Parvalbumin immunoreactivity: a reliable marker for the effect of monocular deprivation in the rat visual cortex. Neuroscience 51, 749–753.

Chappert-Piquemal, C., Fonta, C., Malecaze, F., Imbert, M., 2001. Ocular dominance columns in the adult New World monkey *Callithrix jacchus*. Visual Neurosci. 18, 407–412.

Chard, P.S., Bleakman, D., Christakos, S., Fullmer, C.S., Miller, R.J., 1993. Calcium buffering properties of calbindin D28k and parvalbumin in rat sensory neurones. J. Physiol. (London) 472, 341–357.

Chino, Y.M., 1995. Adult plasticity in the visual system. Can. J. Physiol. Pharmacol. 73, 1323–1338.

Darian-Smith, C., Gilbert, C.D., 1994. Axonal sprouting accompanies functional reorganization in adult cat striate cortex. Nature 368, 737–740.

Darian-Smith, C., Gilbert, C.D., 1995. Topographic reorganization in the striate cortex of the adult cat and monkey is cortically mediated. J. Neurosci. 15, 1631–1647.

DeFelipe, J., Jones, E.G., 1992. High-resolution light and electron

microscopic immunocytochemistry of colocalized GABA and calbindin D-28K in somata and double bouquet cells axons of monkey somatosensory cortex. Eur. J. Neurosci. 4, 46–60.
DeFelipe, J., Hendry, S.H., Jones, E.G., 1989a. Visualization of chandelier cell axons by parvalbumin immunoreactivity in monkey cerebral cortex. Proc. Natl. Acad. Sci. U. S. A. 86, 2093–2097.
DeFelipe, J., Hendry, S.H., Jones, E.G., 1989b. Synapses of double bouquet cells in monkey cerebral cortex visualized by calbindin immunoreactivity. Brain Res. 503, 49–54.
Demeulemeester, H., Vandesande, F., Orban, G.A., Heizmann, C.W., Pochet, R., 1989. Calbindin D-28K and parvalbumin immunoreactivity is confined to two separate neuronal subpopulations in the cat visual cortex, whereas partial coexistence is shown in the dorsal lateral geniculate nucleus. Neurosci. Lett. 99, 6–11.
Fiorani, J.R.M., Gattass, R., Rosa, M.G.P., Sousa, A.P.B., 1989. Visual area MT in the *Cebus* monkey: location, visuotopic organization, and variability. J. Comp. Neurol. 287, 98–118.
Fonta, C., Chappert, C., Imbert, M., 1997. *N*-Methyl-D-aspartate subunit R1 involvement in the postnatal organization of the primary visual cortex of *Callithrix jacchus*. J. Comp. Neurol. 386, 260–276.
Freese, C.H., Oppenheimer, J.H., 1981. The capuchin monkeys, genus *Cebus*. In: Coimbra-Filho, A.F., Mittermeier, R.A. (Eds.), Ecology and Behavior of Neotropical Primates. Academia Brasileira de Ciências, pp. 331–390.
Gattass, R., Gross, C.G., 1981. Visual topography of the striate projection zone in the posterior superior temporal sulcus (MT) of the macaque. J. Neurophysiol. 46, 621–638.
Gattass, R., Gross, C.G., Sandell, J.H., 1981. Visual topography of V2 in the macaque. J. Comp. Neurol. 201, 519–539.
Gattass, R., Sousa, A.P.B., Rosa, M.G.P., 1987. Visual topography of V1 in the *Cebus* monkey. J. Comp. Neurol. 259, 529–548.
Gattass, R., Sousa, A.P.B., Gross, C.G., 1988. Visuotopic organization and extent of V3 and V4 of the macaque. J. Neurosci. 8, 1831–1845.
Gattass, R., Rosa, M.G.P., Sousa, A.P.B., Pinon, M.C.G., Fiorani Jr., M., Neuenschwander, S., 1990. Cortical streams of visual information processing in primates. Braz. J. Med. Biol. Res. 23, 375–393.
Gilbert, C.D., Wiesel, T.N., 1992. Receptive field dynamics in adult primary visual cortex. Nature 356, 150–152.
Goodchild, A.K., Martin, P.R., 1998. The distribution of calcium-binding proteins in the lateral geniculate nucleus and visual cortex of a New World monkey, the marmoset, *Callithrix jacchus*. Visual Neurosci. 15, 625–642.
Gutierrez, C., Cusick, C.G., 1994. Effects of chronic monocular enucleation on calcium binding proteins calbindin-D28k and parvalbumin in the lateral geniculate nucleus of adult rhesus monkeys. Brain Res. 651, 300–310.
Heizmann, C.W., Hunziker, W., 1991. Intracellular calcium-binding proteins: more sites than insights. Trends Biochem. Sci. 16, 98–103.
Hendry, S.H., Bhandari, M.A., 1992. Neuronal organization and plasticity in adult monkey visual cortex: immunoreactivity for microtubule-associated protein 2. Visual Neurosci. 9, 445–459.
Hendry, S.H., Carder, R.K., 1993. Neurochemical compartmentation of monkey and human visual cortex: similarities and variations in calbindin immunoreactivity across species. Visual Neurosci. 10, 1109–1120.
Hendry, S.H., Jones, E.G., 1986. Reduction in number of immunostained GABAergic neurones in deprived-eye dominance columns of monkey area 17. Nature 320, 750–753.
Hendry, S.H., Jones, E.G., Emson, P.C., Lawson, D.E., Heizmann, C.W., Streit, P., 1989. Two classes of cortical GABA neurons defined by differential calcium binding protein immunoreactivities. Exp. Brain Res. 76, 467–472.
Horton, J.C., Hocking, D.R., 1998. Monocular core zones and binocular border strips in primate striate cortex revealed by contrasting effects of enucleation, eyelid suture, and retinal laser lesions on cytochrome oxidase activity. J. Neurosci. 18, 5433–5455.
Ichida, J.M., Rosa, M.G., Casagrande, V.A., 2000. Does the visual system of the flying fox resemble that of primates? The distribution of calcium-binding proteins in the primary visual pathway of *Pteropus poliocephalus*. J. Comp. Neurol. 417, 73–87.
Johnson, J.K., Casagrande, V.A., 1995. Distribution of calcium-binding proteins within the parallel visual pathways of a primate (*Galago crassicaudatus*). J. Comp. Neurol. 356, 238–260.
Jones, E.G., Hendry, S.H., 1989. Differential calcium binding protein immunoreactivity distinguishes classes of relay neurons in monkey thalamic nuclei. Eur. J. Neurosci. 1, 222–246.
Kawaguchi, Y., Kubota, Y., 1993. Correlation of physiological subgroupings of nonpyramidal cells with parvalbumin- and calbindin D28K-immunoreactive neurons in layer V of rat frontal cortex. J. Neurophysiol. 70, 387–396.
Le Gros Clark, W.E., 1959. The Antecedents of Man. Edinburgh Univ. Press, Edinburgh.
Matsubara, J.A., Lam, D.Y, Kalil, R.E., Gabelt, B.T., Nork, T.M., Hornan, D., Kaufman, P.L., 2001. The effects of panretinal photocoagulation on the primary visual cortex of the adult monkey. Trans. Am. Ophthalmol. Soc. 99, 33–42.
Mize, R.R., Jeon, C.J., Butler, G.D., Luo, Q., Emson, P.C., 1991. The calcium-binding protein calbindin-D28k reveals subpopulations of projection and interneurons in the cat superior colliculus. J. Comp. Neurol. 307, 417–436.
Mize, R.R., Luo, Q., Butler, G., Jeon, C.J., Nabors, B., 1992a. The calcium-binding proteins parvalbumin and calbindin-D28k form complementary patterns in the cat superior colliculus. J. Comp. Neurol. 320, 243–256.
Mize, R.R., Luo, Q., Tigges, M., 1992b. Monocular enucleation reduces immunoreactivity to the calcium-binding protein calbindin 28 kD in the rhesus monkey lateral geniculate nucleus. Visual Neurosci. 9, 471–482.
Rausell, E., Cusick, C.G., Taub, E., Jones, E.G., 1992. Chronic deafferentation in monkeys differentially affects nociceptive and nonnociceptive pathways distinguished by specific calcium binding proteins and down-regulates γ-aminobutyric acid type A receptors at thalamic levels. Proc. Natl. Acad. Sci. U. S. A. 89, 127–131.
Rosa, M.G.P., 2002. Visual maps in the adult primate cerebral cortex: some implications for brain development and evolution. Braz. J. Med. Biol. Res. 35, 1485–1498.
Rosa, M.G.P., Sousa, A.P.B., Gattass, R., 1988. Representation of the visual field in the second visual area in the *Cebus* monkey. J. Comp. Neurol. 275, 326–345.
Rosa, M.G.P, Gattass, R., Fiorani Jr., M., Soares, J.G.M., 1992. Laminar, columnar and topographic aspects of ocular dominance in the primary visual cortex of *Cebus* monkeys. Exp. Brain Res. 88, 249–264.
Rosa, M.G.P., Schmid, L.M, Calford, M.B., 1995. Responsiveness of cat area 17 after monocular inactivation: limitation of topographic plasticity in adult cortex. J. Physiol. 482, 589–608.
Sengpiel, F., Troilo, D., Kind, P.C., Graham, B., Blakemore, C., 1996. Functional architecture of area 17 in normal and monocularly deprived marmosets (*Callitrix jacchus*). Visual Neurosci. 13, 145–160.
Silvermann, M.S., Tootell, R.G.H., 1987. Modified technique for cytochrome oxidase histochemistry: increased staining intensity and compatibility with 2-deoxyglucose autoradiography. J. Neurosci. Methods 19, 1–10.
Soares, J.G.M, Gattass, R., Souza, A.P., Rosa, M.G., Fiorani, M., Brandao, B.L., 2001. Connectional and neurochemical

subdivisions of the pulvinar in *Cebus* monkeys. Visual Neurosci. 18, 25–41.
Soares, J.G.M, Pereira, A.C., Botelho, E.P., Fiorani, M., Gattass, R., 2005. Differential expression of Zif268 and c-Fos in the primary visual cortex and lateral geniculate nucleus of normal *Cebus* monkeys and after monocular lesions. J. Comp. Neurol. 482, 166–175.
Stichel, C.C, Singer, W., Heizmann, C.W., 1988. Light and electron microscopic immunocytochemical localization of parvalbumin in the dorsal lateral geniculate nucleus of the cat: evidence for coexistence with GABA. J. Comp. Neurol. 268, 29–37.
Tigges, M., Tigges, J., 1991. Parvalbumin immunoreactivity of the lateral geniculate nucleus in adult rhesus monkeys after monocular eye enucleation. Visual Neurosci. 6, 375–382.
Van Brederode, J.F., Mulligan, K.A., Hendrickson, A.E., 1990. Calcium-binding proteins as markers for subpopulations of GABAergic neurons in monkey striate cortex. J. Comp. Neurol. 298, 1–22.